MEASUREMENTS OF THE FRAGMENTATION OF ^{40}Ar, ^{28}Si AND ^{12}C in CH_2, C AND H TARGETS BETWEEN 300 AND 1500 MEV/NUC AT THE BEVALAC

W. R. Webber & J. C. Kish
Space Science Center
University of New Hampshire
Durham, NH 03824

1. Introduction. In the two years since the last cosmic ray conference we have continued our studies of the fragmentation of various nuclei in CH_2 and C targets with the objective of obtaining cross sections in hydrogen for use in the cosmic ray propagation problem. New measurements include ^{56}Fe, where we now have measurements at 6 energies between 300 and 1700 MeV/nuc, ^{12}C where we also have measurements at six energies, ^{28}Si with measurements at three energies and ^{40}Ar where there are measurements at two energies. The ^{56}Fe data has been summarized in a recent paper (Webber, 1984), in this paper we shall report the new data on ^{12}C, ^{28}Si, and ^{40}Ar nuclei and compare it with the earlier semi-empirical predictions.

2. Experimental Details. a) Charge cross sections. The cross sections in H are obtained using the following procedures. 7.5 cm diameter CH_2 and C targets of varying thickness are placed directly in front of a small Cerenkov x total energy telescope. The thickness of the targets is chosen so that the E loss in each type of target is the same. The CH_2 and C targets are alternated with no target. The H cross sections are obtained by a CH_2 - C subtraction; the no target data is subtracted directly from the individual CH_2 and C runs.

The telescope used is a smaller version of the charge isotope telescope we have used to measure primary cosmic rays. It has been described previously (Webber and Brautigam, 1982). The current telescope is similar but contains several significant improvements. The charge module used in this study contains three thin waveshifted CaF_2 scintillators and a 7940 glass waveshifted fused silica Cerenkov counter. The CaF_2 scintillators have better linearity and resolution than the NE102 scintillators used previously and the 7940 Cerenkov radiator has much better resolution than a comparable thickness of 425 lucite. The analysis procedures used to obtain the total interaction cross sections and the relative charge abundances of the fragments have been described previously (Webber and Brautigam, 1982) and will not be repeated here. In Table I we show some of the parameters of the runs reported here along with the total charge changing cross sections measured. In Table II the various individual charge changing cross sections are given.

b) Isotopic cross sections. To obtain the isotopic composition of the fragments, the events for each charge are treated separately. Additional consistency criteria are placed on the output of all counters in the telescope before the stopping E counter. A matrix of events, C vs stopping E, is made which shows the individual mass lines and from which the mass histograms are constructed. The fraction of events for each charge to be associated with each isotope is obtained by summing the appropriate mass histograms. The typical mass resolution obtained with our recent telescope ranges from σ of about 0.15 AMU for ^{16}O to 0.25 AMU for ^{56}Fe. The isotopic cross sections obtained for ^{12}C, ^{28}Si, and ^{40}Ar for hydrogen targets are shown in Table III.

3. Discussion of Results. a) ^{12}C cross sections. The results for Be and B secondaries are shown in Figure 1, along with the semi-empirical predictions of Tsao and Silberberg (1979). The semi-empirical cross sections appear to be an overestimate at all energies - but particularly - below ~ 1 GeV/nuc where the difference is as great as 30% at energies of a few hundred MeV/nuc. Since the B/C ratio is generally used as a reference to determine the path length traversed by cosmic rays as a function of energy, and since ~ 70% of all Be and B are produced by ^{12}C, these new cross sections will lead to a considerably different interpretation of this energy dependence - particularly below 1-2 GeV/nuc.

The isotope fractions we measure for Be and B are in generally much better agreement with the semi-empirical predictions.

b) ^{28}Si and ^{40}Ar. The main feature of our new cross sections for the production of secondary nuclei by these elements is the large excess in the production of secondaries in the Z = 12-17 range over the semi-empirical predictions. This is illustrated in Figure 2 for an average energy ~ 650 MeV/nuc. In some cases, e.g. the production of Mg and Si from ^{40}Ar, this difference is almost a factor of 2! From a study of the semi-empirical cross sections for nuclei of different Z and different neutron excess, we conclude that the semi-empirical formulae probably considerably underestimate the production of secondary nuclei with Z~12-20 from all primary nuclei with Z~14-22, and that the effect we observe is not just associated with the large neutron excess of ^{40}Ar. This will have a very important effect on the secondary production during interstellar propagation of the rarer elements in this charge range such as Al, P, Cl, Ar and K, which in turn will modify the source abundances of these charges that are deduced. A comparable effect will occur for the neutron rich isotopes - such as ^{26}Mg, ^{29}Si, and ^{30}Si and ^{34}S, possibly significantly altering the source abundances deduced for these isotopes as well.

4. Acknowledgements. This work was supported by a HEAO Guest Investigator Grant #NAG-8-451, and also by a NASA Support Grant #NGR-30-002-052.

5. References.

Tsao, C.H., and Silberberg, R., Proc. 16th ICRC, 2, 202, 1979

Webber, W.R., and Brautigam, D.A., Ap.J., 260, 894, 1982

Webber, W.R., paper presented at Workshop on Cosmic Ray & High Energy γ-ray Experiments for the Space Station Era, LSU, Oct., 1984.

6. Figure Captions.

Figure 1. Cross Sections for ^{12}C fragmenting into Be and B nuclei. Data from this work shown as solid circles.

Figure 2. Ratio of cross sections for ^{40}Ar and ^{28}Si fragmentation measured in this work to the semi-empirical predictions of Tsao and Silberberg (1979).

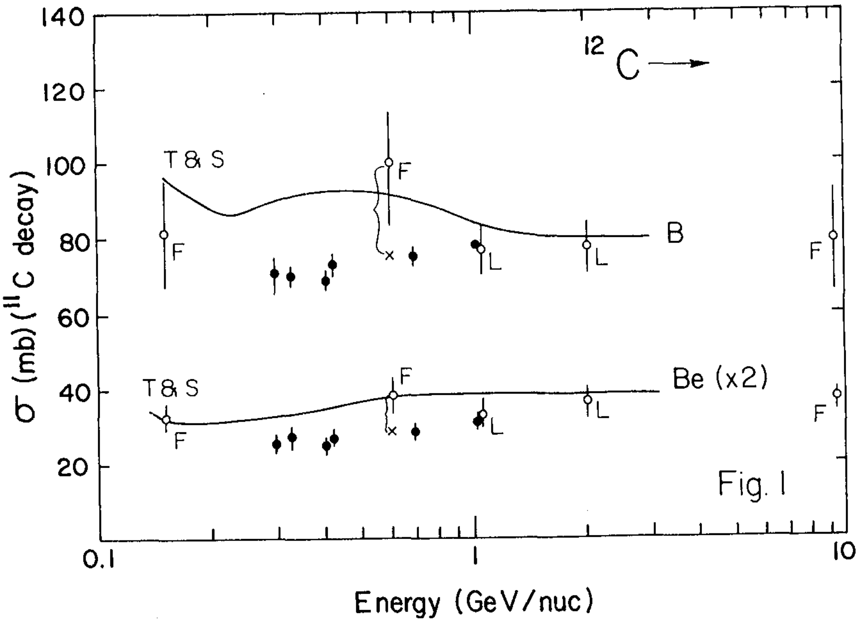

Fig. 1

Table 1

Parameters for BEVALAC Measurements

E (target) (MeV)	Target	(g/cm²)	N_B (x1,000)	N_Z/N_B	(ΔZ Changing) λ(g/cm²)	σ(mb)
			^{12}C beam			
1016	CH_2 =	8.75	417.2	0.6428	19.80	1179
	C =	10.01	387.8	0.6943	27.44	727
	H =	-	-	-	7.36	226
693	CH_2 =	8.75	217.3	0.6468	20.08	1163
	C =	10.01	203.6	0.6962	27.64	721
	H =	-	-	-	7.53	221
412	CH_2 =	6.01	486.3	0.7635	22.28	1044
	C =	7.03	465.9	0.7879	29.56	675
	H =	-	-	-	8.99	185
310	CH_2 =	6.01	235.9	0.7663	22.57	1030
	C =	7.03	233.9	0.7905	29.89	666
	H =	-	-	-	9.14	182
			^{28}S beam			
1296	CH_2 =	6.01	239.0	0.5869	11.44	2037
	C =	7.03	230.0	0.6452	16.11	1229
	H =	-	-	-	4.13	403
770	CH_2 =	6.01	491.0	0.5956	11.77	1980
	C =	7.03	527.1	0.6508	16.44	1215
	H =	-	-	-	4.32	385
603	CH_2 =	6.01	597.6	0.5911	11.61	2004
	C =	7.03	594.2	0.6459	16.15	1235
	H =	-	-	-	4.33	384
			^{40}Ar beam			
792	CH_2 =	6.01	423.7	0.5198	9.19	2532
	C =	7.03	336.6	0.6014	13.83	1436
	H =	-	-	-	3.05	544
521	CH_2 =	5.26	295.3	0.5686	9.29	2501
	C =	6.15	263.0	0.6455	14.05	1419
	H =	-	-	-	3.08	539

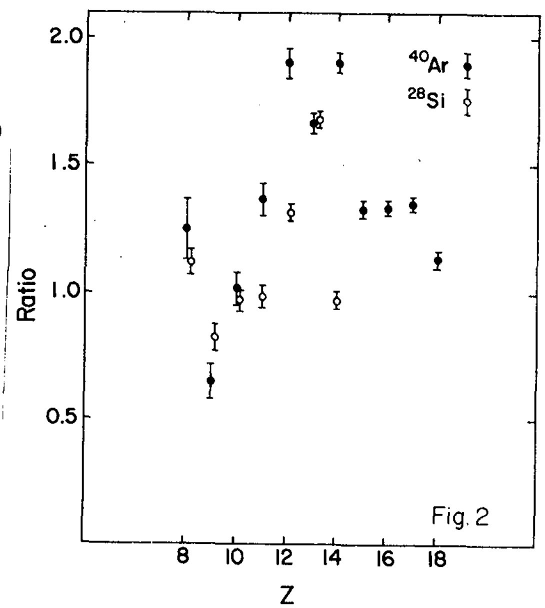

Fig. 2

Table II

Charge Changing Cross Sections In Hydrogen

(σ in mb)

^{12}C

Z	1016 MeV/nuc	693 MeV/nuc	403 MeV/nuc	326 MeV/nuc
B	52.9±1.0	51.3±1.1	45.3±1.0	43.6±1.0
Be	15.8±0.8	13.9±0.8	13.0±0.7	13.8±0.8
Li	30.5±2.0	26.6±2.0	24.6±1.8	27.2±2.2

^{28}Si

Z	1296 MeV/nuc	770 MeV/nuc	503 MeV/nuc
Al	84.0±1.5	86.5±1.5	85.3±1.3
Mg	82.7±1.5	84.6±1.5	88.1±1.3
Na	35.6±0.8	38.1±0.8	42.0±0.8
Ne	35.3±0.8	35.0±0.8	37.1±0.7
Fl	17.2±0.7	17.0±0.7	15.9±0.6
O	33.0±1.0	30.5±1.0	33.6±0.9
N	19.6±0.8	18.6±0.8	19.9±0.8
C	31.2±1.0	26.5±1.0	25.7±0.9

^{40}Ar

Z	792 MeV/nuc	521 MeV/nuc
Cl	136.2±1.6	140.3±1.2
S	94.1±1.2	99.6±0.9
P	66.8±1.0	73.5±0.8
Si	74.0±1.0	75.0±0.8
Al	45.6±0.8	47.4±0.6
Mg	41.5±0.8	37.0±0.6
Na	22.1±0.6	20.9±0.5
Ne	15.8±0.5	8.3±0.4
Fl	6.8±0.4	3.3±0.4
O	11.7±0.6	5.1±0.4

Table III

Isotopic Cross Sections
(σ in mb)

	^{12}C 403 MeV/nuc
^{11}C	27.6±1.2
^{10}C	1.0±0.2
^{11}B	30.9±1.2
^{10}B	15.9±1.0
^{10}Be	1.4±0.3
^{9}Be	4.8±0.4
^{7}Be	7.0±0.7

	^{28}Si 770 MeV/nuc
^{27}Si	31.3±0.9
^{26}Si	1.4±0.3
^{27}Al	53.0±1.2
^{26}Al	32.0±1.1
^{25}Al	1.6±0.3
^{27}Mg	1.9±0.4
^{26}Mg	16.3±0.8
^{25}Mg	29.0±1.2
^{24}Mg	35.6±1.3
^{23}Mg	4.1±0.9
^{25}Na	0.5±0.2
^{24}Na	5.2±1.0
^{23}Na	17.8±0.9
^{22}Na	11.1±0.8
^{21}Na	1.0±0.3
^{23}Ne	0.5±0.2
^{22}Ne	6.1±0.7
^{21}Ne	12.8±1.1
^{20}Ne	14.9±1.1
^{19}Ne	3.0±0.5

	^{40}Ar 521 MeV/nuc
^{39}Ar	65.6±1.6
^{38}Ar	30.3±0.9
^{37}Ar	1.7±0.3
^{39}Cl	31.6±1.0
^{38}Cl	23.0±0.8
^{37}Cl	48.2±1.2
^{36}Cl	27.8±0.9
^{35}Cl	10.7±1.0
^{38}S	0.6±0.2
^{37}S	3.1±0.4
^{36}S	15.9±0.9
^{35}S	28.4±1.0
^{34}S	43.1±1.2
^{33}S	13.9±1.1
^{32}S	1.2±0.6
^{35}P	0.4±0.2
^{34}P	5.1±0.7
^{33}P	21.7±1.0
^{32}P	28.3±1.1
^{31}P	16.4±0.9
^{30}P	1.2±0.5

	^{40}Ar 521 MeV/nuc
^{32}Si	1.4±0.3
^{31}Si	9.8±0.9
^{30}Si	36.2±1.2
^{29}Si	22.3±0.9
^{28}Si	5.6±0.5
^{30}Al	0.7±0.2
^{29}Al	7.5±0.8
^{28}Al	14.8±0.7
^{27}Al	22.5±1.0
^{26}Al	4.6±0.6
^{27}Mg	2.2±0.5
^{26}Mg	14.7±0.9
^{25}Mg	13.8±0.9
^{24}Mg	6.4±0.7